Available online at www.sciencedirect.com

ScienceDirect

Physics Procedia 50 (2013) 261 – 266

Physics Procedia

International Federation for Heat Treatment and Surface Engineering 20th Congress
Beijing, China, 23-25 October 2012

Chrome-free Samarium-based Protective coatings for Magnesium Alloys

Legan Hou, Xiufang Cui, Yuyun Yang, Lili Lin , Qiang Xiao, Guo Jin*

Institute of Surface/Interface Science and Technology, School of Materials Science and Chemical Engineering, Harbin Engineering University, Harbin 150001, China

Abstract

The microstructure of chrome-free samarium-based conversion coating on magnesium alloy was investigated and the corrosion resistance was evaluated as well. The micro-morphology, transverse section, crystal structure and composition of the coating were observed by scanning electron microscopy (SEM), X-ray diffraction (XRD) , energy dispersive spectroscopy (EDS) and X-ray photoelectron spectroscopy (XPS), respectively. The corrosion resistance was evaluated by potentiodynamic polarization curve and electrochemical impedance spectroscopy (EIS). The results reveal that the morphology of samarium conversion coating is of crack-mud structure. Tiny cracks distribute in the compact coating deposited by samarium oxides. XRD, EDS and XPS results characterize that the coating is made of amorphous and trivalent-samarium oxides. The potentiodynamic polarization curve, EIS and OCP indicate that the samarium conversion coating can improve the corrosion resistance of magnesium alloys.

Keywords: microstructure; corrosion; samarium; conversion coating; morphology

1. Introduction

The lanthanides ions of rare earth elements, as Ce^{3+}, La^{3+}, Sm^{3+}, Nd^{3+}, Pr^{3+}, have a lower toxicity and are considered as the best candidate for replacing the hexavalent chromium compounds of high toxicity. In previous work, lanthanum and cerium conversion coating are well known to inhibit the corrosion processes on some alloys such as aluminium alloys (Campestrini et al., 2004, Heller et al., 2010, Chen et al., 2009), magnesium alloys (Rudd et al., 2000, Yang et al., 2008, Wang et al., 2009, Yang et al., 2009, Montemor et al., 2007, Dabala et al., 2003) and zinc (Montemor et al., 2002, Aramaki, 2001). But there is no paper reported on samarium conversion coating.

* Corresponding author. Tel.: +86-451-82589660.
E-mail address: jinguo@hrbeu.edu.cn.

doi:10.1016/j.phpro.2013.11.041

Samarium (Sm) is discovered by L. Boisbaubran. It mainly consists in the monazite and bastnaesite. The application of samarium reagent in organic synthesis is one of the actively investigative fields in organic synthetic methodology recently. However, samarium used as protective and non-toxic chemical conversion coating is rarely studied.

In this article, newly developed environmentally surface treatment was proposed based on Sm^{3+}as alternatives to toxic chromate-based systems. Micro-morphology, microstructure and corrosion performance of the samarium conversion coating were studied according to priority. Surface examinations were performed by SEM, EDS, XPS and XRD. Corrosion behaviors of the samarium coating on AZ91 surface in 3.5% NaCl solution were carried out by OCP, potentiodynamic polarization curve and EIS.

2. Experimental methods

The neodymium conversion coating was obtained on the matrix of die-cast AZ91. Test samples (15mm×10mm×5mm) were polished using waterproof abrasive paper from 360 grits to 2500 grits, then fine polished using diamond paste of 3.5 μm, and then they were degreased with absolute ethanol in ultrasonic bath for 15 min and subsequently dried by cold air in room temperature.

The optimal technical parameters determined by orthogonal experiment were the neodymium nitrate, $Sm(NO_3)_3$, with concentrations of 5g/L, and 20 ml/L of hydrogen dioxide solution, H_2O_2 (Fisher Scientific, 30%) used as the accelerant. The obtained solution had been mixed for 5 minutes with a magnetic stirrer prior to deposition. The samples were immersed in the conversion solution at 50℃ for 20 minutes. After all these treatments, the samples were thoroughly rinsed with deionized water and then dried in cold air.

The micro-morphology was observed by a FEI Quant200 SEM equipped with EDS. The crystal structure of the conversion coating was studied by XRD. XPS was employed to determine the Oxidation state of samarium at the surface of magnesium alloys. The X-ray source was monochromatized AlKα radiation. The accelerating voltage was 12 KV.

The anticorrosion performance was evaluated by recording the corrosion potential and corrosion current density of the samples in 3.5% sodium chloride (NaCl) solution upon immersion, which was conducted on a CHI660B electrochemical workstation. The electrochemical cell used a classic three-electrode system which consists of a reference electrode (a saturated calomel electrode), a counter electrode (a platinum foil) and a working electrode. The potentiodynamic polarization curves were performed at a scanning rate of 1 mV/s. OCP and EIS measurements were carried out at corrosion potential in a frequency range between 0.01 Hz and 100000 Hz using a 10 mV amplitude perturbation.

3. Results and discussions

3.1. Morphology, composition and structure of conversion coating

SEM was used to reveal the morphology of the samarium conversion coating. As shows in Fig. 1, the tiny and thick cracks distribute in the compact coating were obtained at the optimal preparation process. The coating has being forming by depositing amorphous and trivalent-samarium oxides which were determined via XRD, XPS and EDS measurements. To identify the composition of the corrosion products, EDS is employed to characterize the elements of samarium conversion coating. In Fig.1 (b), the element weight percentage (wt. %) and atomic percentage (at. %) of samarium conversion coating are listed. It is shown as following: O (32.24 at. %) dominated in the coating, Mg was 55.31 at. %, Al was3.09 at.% and Sm was 9.36 at.% in the samarium coating, orderly. EDS is consistent with the phenomenon revealed by SEM. The samarium weight percentage (wt. %) is nearly half within the conversion coating.

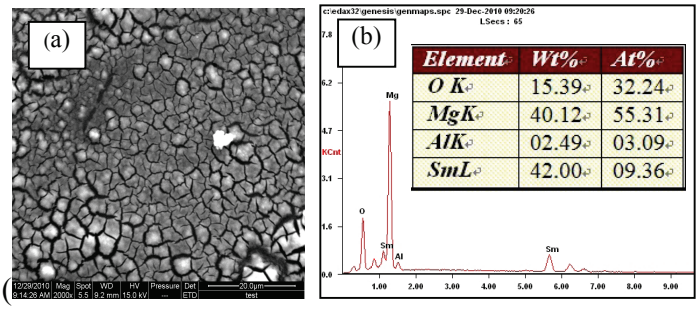

Fig. 1 Morphology (a) and composition (b) of conversion coating on magnesium alloy

The morphology of the transverse section of conversion specimen is shown in Fig. 2. It can be seen that the white area of the Fig.2 is samarium conversion coating and the gray one is matrix. The coating combines with Mg alloys tightly and the thickness of samarium conversion coating is about 2-3 μm .It is clear that the layer is compact with less and tiny cracks, but without though cracks. The layer nearby matrix has no-through cracks and is covered by a compact outer layer. The specific structure of samarium conversion coating keeps the easy corroded magnesium alloys away from corrosion medium in ambient.

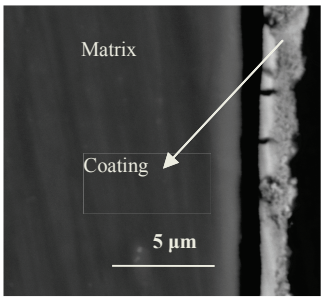

Fig. 2 Transverse section morphology of the samarium conversion coating

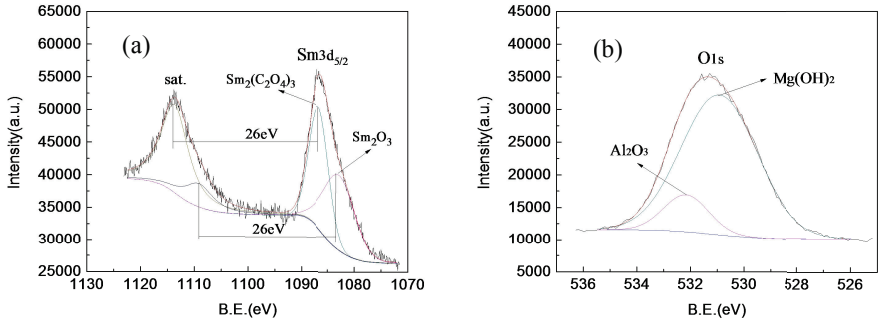

Fig. 3 XPS patterns of samarium conversion coating: (a) the high resolution spectra of Sm, (b) the high resolution spectra of O

In Fig. 3, the XPS spectra of the samarium conversion coating is depicted. The high resolution spectrum of single element is shown in Fig. 3a and b. As shown in Fig. 3 (a), the Sm $3d_{5/2}$ peak is measured elaborately. Samarium has only one stable oxidation state, Sm^{3+}, indicating that the conversion coating consists of Sm_2O_3 and $Sm_2(C_2O_4)_3$ (formed by Sm_2O_3 carbonization). The binding energy of the oxide and carboxide are at 1084.16eV and 1086.49 eV.

Binding energy of two peaks is almost coincident with the reference value (1084.30 eV and 1085.50 eV). O 1s peak is assigned to a large part of $Mg(OH)_2$and a few of Al_2O_3 which are labeled in Fig. 2 (b). All these research reveal that the cerium conversion coating is mainly composed of Sm_2O_3, $Sm_2(C_2O_4)_3$, $Mg(OH)_2$ and Al_2O_3.

Fig. 4 displays the XRD patterns of the coated and uncoated samples. Compared with the uncoated sample, the XRD pattern of the coated sample has an obvious bread-peak; the appearance of the bread-shaped peak from 24° to 29° indicates that the formed samarium conversion coating on the matrix was of amorphous structure. Samarium peaks, like at 33°, 36° and 64°, broads the matrix peaks. Results of the XRD patterns in Fig. 3 corresponded with the results from SEM and EDS.

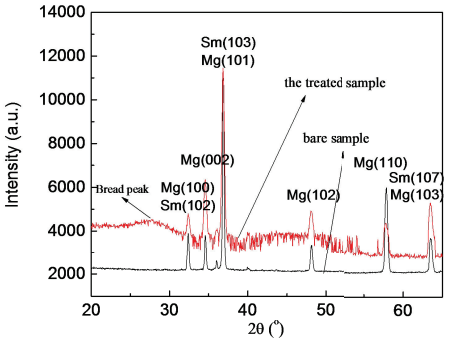

Fig.4 XRD patterns of samarium conversion coating

3.2 Corrosion resistance of conversion coating

The electrochemical experiments are employed to characterize corrosion resistance of samarium conversion coating. The change of open circuit potential (OCP) can be used to monitor the chemical stability and the corrosion process of specimens during immersion period. Evolution of OCP for the samarium conversion coating and the untreated sample in 3.5 % NaCl solution is shown in Fig. 5 (a). OCP of the untreated sample keeps at a stable value of -1.55 V which is lower than that of the treated one holding at about -1.50 V for 360s immersion period. The OCP curve of treated sample tends to a more positive potential after 260 s. A more positive OCP implies a good corrosion resistance (Huang et al., 2004). The equilibrium OCP of samarium conversion coating indicates that the stability of the coating has a better anticorrosion property than the bare substrate. Therefore, the corrosion resistance of magnesium alloy can be improved through the cerium conversion treatment.

In order to evaluate the corrosion inhibition effect of samarium conversion coating, EIS was done for the samples after OCP stabilization. In Fig. 5 (b), the impedance spectra of the untreated magnesium electrode and the samarium-treated electrode were recorded in 3.5% NaCl solution after about 6 min immersion for OCP measure. EIS of the treated sample and the untreated one both shows a capacitive loop in the high frequency range and an inductive loop in the intermediate frequency range. The total impedance value of the treated sample was 2.5×10^3 $\Omega\cdot cm^2$ and that of the untreated one was $1.3\times10^3\Omega\cdot cm^2$. The diameter of the capacitive loop is associated with the charge-transfer resistance and subsequently, with the corrosion resistance (Xue et al., 2011, Liu et al., 2010). Therefore, the higher charge-transfer resistance involves the better the corrosion resistance. EIS plots in Fig. 5 (b) clearly reveal a larger Rp value for treated specimen than for untreated specimen immersed in 3.5% NaCl solution. So, the samarium treated sample has a better corrosion resistance than the bare sample.

Potentiodynamic polarization curve was employed to investigate corrosion resistance of the sample. In a typical polarization curve, lower corrosion densities correspond to lower corrosion rates and better corrosion resistance (Lévesque et al., 2008).The sample immersed in 3.5 wt. % NaCl aqueous at room temperature after 30 min. The potentiodynamic polarization curves for the treated and untreated one are plotted in Fig. 5 (c). Samarium conversion coating on magnesium alloy decreases the corrosion current density (Icorr) about two orders of magnitude, compared with the substrate. Partially blocking the cathodic reaction and shifting the polarization curves toward lower current density values. It can also be obviously seen that the corrosion potential (Ecorr) of the coating was

about 350 mV higher than that of the substrate. These results demonstrated that the anticorrosion capability of the magnesium alloys had been increased through the neodymium conversion treatment.

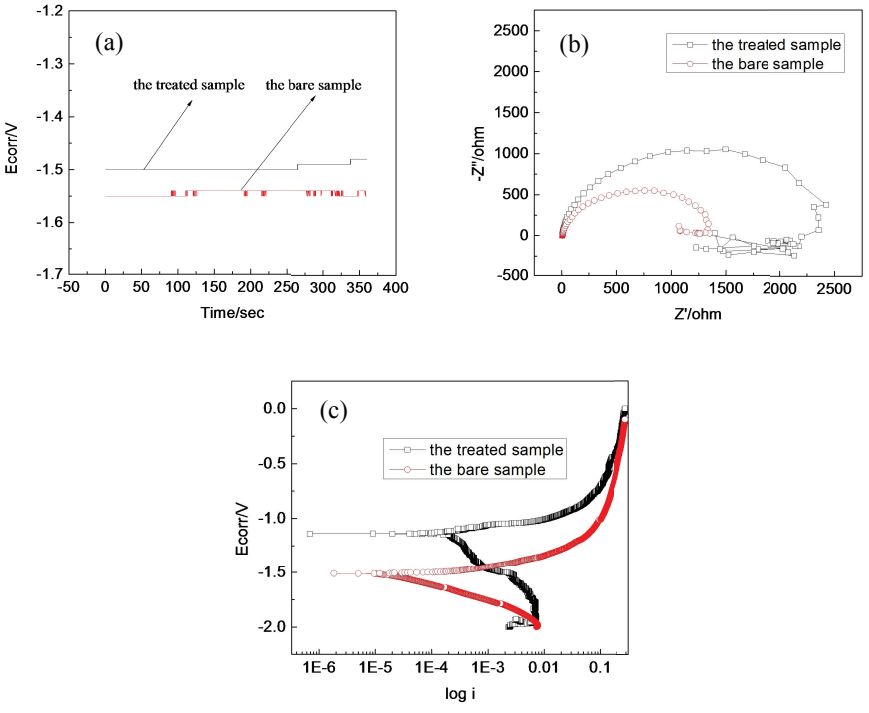

Fig. 5 The open circuit potential, EIS spectra and potentiodynamic curve of the treated and untreated samples in 3.5 % NaCl solution

4. Conclusion

(1) The samarium conversion coating is a compact coating with crack-mud morphology.

(2) The coating is mainly made of amorphous samarium oxides.

(3) The electrochemical experiments indicate that the corrosion resistance is improved through the samarium conversion treatment.

Acknowledgement

This work is financially supported by the National Basic Research Program of China (973 Program) (No. 2011CB013404) and National Natural Science Foundation of China (Nos. 51375106, 51275105).

.

References

Campestrini P., Terryn H., Hovestad A., Wit J., 2004. Formation of a cerium-based conversion coating on AA2024: relationship with the microstructure. Surf. Coat. Technol. 176, 365-381.

Heller D., Fahrenholtz W., Keefe M., 2010. The effect of post-treatment time and temperature on cerium-based conversion coatings on Al 2024-T3. Corros. Sci. 52, 360-368.

Chen D., Li W., Gong W., Wu G., Wu J., 2009. Microstructure and formation mechanism of Ce-based chemical conversion coating on 6063 Al alloy. Trans. Nonferrous Met. Soc. China. 19, 592-600.

Rudd A., Breslin C., Mansfeld F., 2000. The corrosion protection afforded by rare earth conversion coatings applied to magnesium. Corros. Sci. 42, 275-288.

Yang L., Li J., Yu X., Zhang M., Huang X., 2008. Lanthanum-based conversion coating on Mg–8Li alloy. Appl. Surf. Sci. 255, 2338-2341.

Wang C., Zhu S., Jiang F., Wang F., 2009. Cerium conversion coatings for AZ91D magnesium alloy in ethanol solution and its corrosion resistance. Corros. Sci. 51, 2916-2923.

Yang X., Wang G., Dong G., Gong F., Zhang M., 2009. Rare earth conversion coating on Mg–8.5Li alloys. J. Alloys. Compd. 487, 64-68.

Montemor M., Simoes A., Carmezim M., 2007. Characterization of rare-earth conversion films formed on the AZ31 magnesium alloy and its relation with corrosion protection. Appl. Surf. Sci. 253, 6922-6931.

Dabala M., Brunelli K., Napolitani E., Magrini M., 2003. Cerium-based chemical conversion coating on AZ63 magnesium alloy. Surf. Coat. Technol. 172, 227-232.

Montemor M., Simoes A., Ferreira M., 2002. Composition and corrosion behaviour of galvanised steel treated with rare-earth salts: the effect of the cation. Prog. Org. Coat. 44, 111-120.

Aramaki K., 2001. Treatment of zinc surface with cerium (III) nitrate to prevent zinc corrosion in aerated 0.5 M NaCl. Corror. Sci. 43, 2201-2215.

Huang Y.S., Zheng X.T., Hu X.F., Liu F.M., 2004. Corrosion resistance properties of electroless nickel composite coatings. Electrochim. Acta. 49, 4313-4319.

Xue D., Yun Y., Mark J., Shanov V., 2011. Corrosion protection of biodegradable magnesium implants using anodization. Mater. Sci. Eng. C. 31, 215-223.

Liu W., Cao F., Chen A., Chang L., Zhang J., Cao C., 2010. Corrosion behaviour of AM60 magnesium alloys containing Ce or La under thin electrolyte layers. Part 1: Microstructural characterization and electrochemical behaviour. Corros. Sci. 52, 627-638.

Lévesque J., Hermawan H., Dubé D., Mantovani D., 2008. Design of a pseudo-physiological test bench specific to the development of biodegradable metallic biomaterials. Acta. Biomater. 4, 284-295.